Published in Journal of Structural Geology 18, issue 6 753-764, 1996
which should be used for any reference to this work

Shear zone patterns and strain distribution at the scale of a Penninic nappe: the Suretta nappe (Eastern Swiss Alps)

DIDIER MARQUER, NATHALIE CHALLANDES and THIERRY BAUDIN

Geological Institute, E. Argand 11, CH2007, Neuchâtel, Switzerland

Abstract—Shear zone patterns within the Suretta nappe of the Swiss Alps are studied in order to understand finite strain and bulk tectonic displacements. The Suretta nappe is chosen for two main reasons; the availability of late Variscan granites deformed during Alpine tectonics only, and because of continuous outcrop from bottom to top of the nappe.

This Alpine nappe recorded two major ductile deformation phases, which developed under low-grade metamorphic conditions. The analysis of shear zone patterns in the Roffna granite reveals that the first deformation is well developed in the entire nappe; the second deformation, however, is more localized in the lower and upper parts. The bulk asymmetry of the shear zone patterns confirms the kinematics recorded by other Penninic nappes in this area: first a stacking of the nappe towards the NW, followed by the top to the E shearing during post-thickening extensional tectonics. The shear zone patterns and strain distribution allow us to deduce kinematics at the nappe scale.

INTRODUCTION

Heterogeneous deformation in basement rocks, especially in those with an initially homogeneous and isotropic structure (e.g. granites), is often expressed by anastomosing shear zones surrounding lenses of weakly deformed rocks (Mitra 1978, 1979, Ramsay 1979, Bell 1981, Choukroune & Gapais 1983, Marquer 1991). At all scales, the previous structures and textures of these basement rocks are preserved within weakly deformed lenses limited by shear zones (Marquer 1991). At a bulk scale, shear zone patterns have been used as qualitative shear criteria and strain markers (Gapais *et al.* 1987). Recently, shear zones have also been used as indicators of palaeostress directions (Srivastava *et al.* 1991). In this paper, the study of the shear zone patterns is performed to estimate the geometry and orientation of the principal finite strain axes and to deduce the bulk tectonic displacements of a Penninic nappe. This analysis of shear zone patterns and strain distribution at the nappe scale give new information about the deformation of the continental lithosphere during mountain building processes.

Since Argand's work (1911, 1916) in the Western Alps, the overall geometry of the Penninic nappes seems to be well established. Recent studies on nappe geometry and basement-cover relationships (see Escher *et al.* 1993) described these nappes as large recumbent folds, referred to as 'ductile basement fold nappes'. On the other hand, recent structural and seismic investigations in the eastern part of the Alps described the nappe geometry as due to thrust tectonics and post-nappe refolding (Schmid *et al.* 1990, Schreurs 1993). After a review of the tectono-metamorphic evolution in this part of the Alps derived from the Briançonnais palaeographic domain, our paper focuses on the internal deformation of a particular basement nappe, the Suretta nappe, in order to understand its large scale deformation mechanisms and kinematics using shear zone patterns. This famous Alpine nappe belongs to the upper Penninic domain in the eastern part of the Central Alps (Trümpy 1980).

In order to test the method of shear zone pattern analysis (Gapais *et al.* 1987) in a basement nappe, the Suretta nappe has been chosen for two main reasons: the occurrence of a late Variscan granite deformed during Alpine tectonics only; and the occurrence of continuous outcrops from top to bottom of this nappe. From a methodological point of view, the study of a late Variscan granite is favourable because (1) Alpine structures can be studied without interference or disturbance due to previously acquired structures, and (2) in the initial state, granites can be considered as relatively homogeneous and isotropic in large volumes, unlike the intruded basement rocks which present a strong planar anisotropy. This paper deals only with the shear zone geometry and kinematic analysis of the main ductile deformation of the late Variscan Roffna granite in the Suretta basement.

GEOLOGICAL SETTING OF THE BRIANÇONNAIS TERRANES

Early cartographic and petrological works (Staub 1916, 1924, Wilhelm 1933, Grünenfelder 1956, Streiff *et al.* 1976), and recent detailed mapping and stratigraphic observations (Suretta nappe: Milnes *et al.* 1978; Schams nappes: Schmid *et al.* 1990, Schreurs 1993; Tambo nappe: Baudin *et al.* 1993, Mayerat 1994; Suretta cover: Baudin *et al.* 1995) define the following structural units in this part of the Alps (Figs. 1 and 2). The stacking of

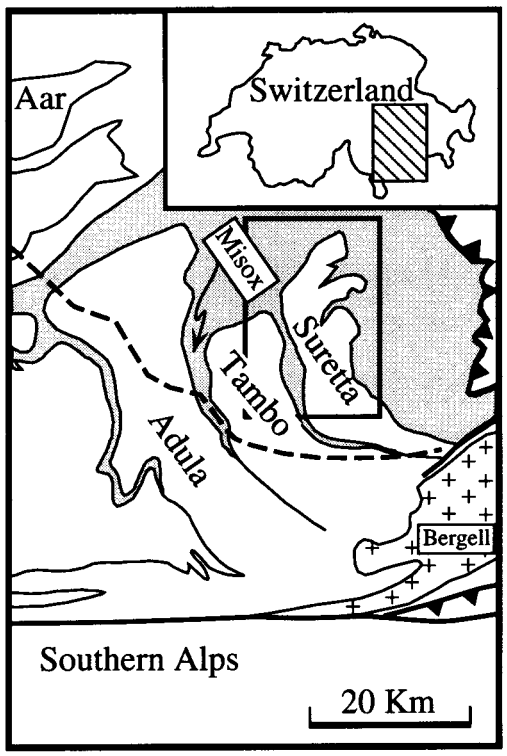

Fig. 1. Simplified geological map of the Eastern Penninic domains illustrating the location of the area studied. Dashed line: staurolit isograd after Frey *et al.* 1979, 1980.

the Adula, Tambo and Suretta nappes results from early Tertiary crustal stacking (Marquer *et al.* 1994). A narrow suture, the so-called Misox zone, separates the south European margin (Adula nappe) from the Briançonnais Tambo and Suretta nappes (Fig. 1). The Misox zone constitutes the southern extremity of the Schistes Lustrés, the Ucello units, which belong to the Valaisan zone (Steinmann 1994) (Fig. 2). During the early Palaeogene, this zone was subducted below the Tambo and Suretta northern Briançonnais realm (Marquer *et al.* 1994). The Mesozoic sediments of the Schams nappes are wrapped around the front of the crystalline basement nappes (Fig. 2). This large scale structural shape, enveloping Tambo and Suretta nappes (Fig. 3), is described as the Niemet–Beverin post-nappe fold in many works (Milnes *et al.* 1978, Schmid *et al.* 1990, Schreurs 1993).

The thin crystalline slivers of Tambo and Suretta, about 3–4 km thick, are mainly composed of polycyclic basement (amphibolites, paragneisses, orthogneisses) intruded by a large magmatic complex, the Roffna granite (Fig. 2). Recent mapping and petrographical observations emphasize that these igneous rocks consist of late Variscan intrusions, probably Permian in age. Their chemical composition and textures are close to those of rhyolitic–granitic rocks and they are associated with volcanic effusives (metatuffs), lying unconformably on the basement of both Tambo and Suretta nappes. This monocyclic Permian volcanoclastic cover progressively grades into conglomerates, subsequently metamorphosed into chlorito–albitic gneiss. It is followed upwards by pure quartzite, probably Scythian in age. A strongly reduced carbonate series, with polygenic breccia, lying unconformably on the older sediment or directly on the basement, exhibits a type of sedimentation comparable to Ultra-Briançonnais terranes. The Starlera nappe, recently defined as an early cover décollement (Baudin *et al.* 1995), tectonically overlies either the reduced autochtonous cover or the basement of Tambo and Suretta units (Figs. 2 and 3). This thrust slice is often underlain by 'cargneules' and consists from bottom to top of Triassic banded marbles and dolomites, dark strong smelling marbles, massive white marbles, calcschists and polygenic breccias, typical for the internal Briançonnais. In the Splügen zone located between Tambo and Suretta units, the Suretta nappe directly overlies the Starlera nappe (Figs. 2 and 3).

TECTONIC SETTING OF THE EASTERN PENNINIC ALPS

Recent structural analyses and seismic investigations (Suretta nappe: Milnes *et al.* 1978, Schmid *et al.* 1990, Schreurs 1993; Tambo: Baudin *et al.* 1993, Mayerat, 1994; Suretta cover: Baudin *et al.* 1995; NFP-20-East seismic lines: Pfiffner *et al.* 1988, 1990, Frei *et al.* 1989) and tectonic models (Merle *et al.* 1989, Schmid *et al.* 1990, Marquer *et al.* 1994, Merle 1994) gave different Tertiary tectonic evolutions for this area. There are some disagreements in these models concerning D_2 deformation events and associated bulk kinematics. According to Marquer *et al.* 1994, the Alpine deformation history of this area may be summarized as follows.

During Tertiary convergent tectonics, four Alpine deformation phases are distinguished. The burying tectonics due to subduction of the thinned continental Briançonnais crust underneath the Austroalpine–Apulian plate is identified as D_1 deformation. D_1 is associated with a strong SSE–NNW stretching lineation and a top to the NNW shearing (Fig. 4). Estimates of the P–T conditions are based on phengitic substitution (Massonne & Schreyer 1987) in D_1 mylonitic foliations and systematically show HP–LT metamorphic conditions. For example, metamorphic conditions of about 12 kb and 500°C are reached in the Tambo nappe (Baudin *et al.* 1993). Ahead of the Tambo and Suretta basement, the pile of crystalline and sedimentary slabs (Ucello, Areua, Schams, Vignone) represents an accretionary wedge particularly well-developed in the northern Penninic schistes lustrés and flysch (Figs. 2 and 3) (Steinmann 1994). The overall geometry of the frontal slices is related to the closure of the Valais trough. The D_1 ductile Alpine deformation is linked to the progressive Eocene stacking of the Adula, Tambo and Suretta nappes towards the NNW and is associated with NW–SE oriented stretching lineations in the Suretta nappe (Fig. 4).

The D_2 deformation is a ductile and heterogeneous deformation, linked with an W–E stretching lineation (Fig. 4). Most of the D_2 mylonitic zones cross-cut pre-

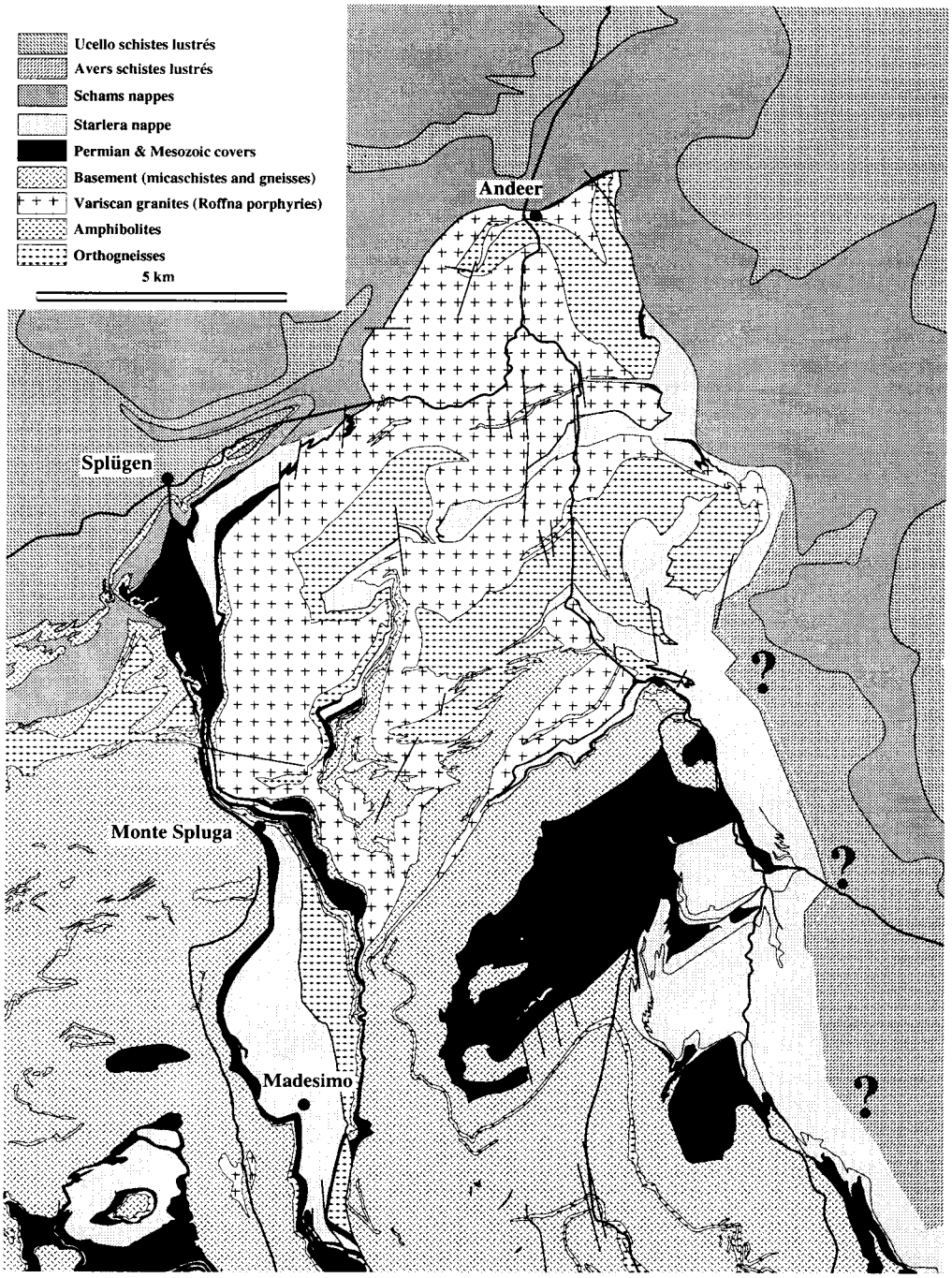

Fig. 2. Geological map of the frontal part of the Suretta nappe: original geological survey of the Suretta and Tambo nappes by the authors (1992–1994 field seasons), geological boundaries of Ucello and Schams units from Schreurs (1993). The contact between Avers- autochthonous Mesozoic cover of Suretta is not actually well-defined.

vious contacts and indicate top to the East shearing. As a consequence of the subvertical shortening between subhorizontal D_2 shear planes (Baudin *et al.* 1993), the gently SE-dipping D_1 foliation and pre-Alpine foliation previously steeply dipping towards the SE underwent strong SE vergent folding (D_2), the angles between the mainly N70 directed fold axes and the E–W stretching lineations being very small (Fig. 4). The rheological contrast between basement and cover appears to have been very low during D_2 deformation. This leads to a very similar style of heterogeneous deformation affecting both basement and cover. The phengitic substitution values measured in the D_2 mylonites or in the D_2 shear bands indicate pressures progressively decreasing with time associated with a slight decrease of temperature. For example, a progressive decrease of pressure and temperature from 11 to 5Kb and 550 to 500°C is recorded at the bottom of the Tambo nappe (Baudin & Marquer 1993) and from 10 to 5Kb at 400–450°C in the Roffna granite (work in preparation). This tectono-metamorphic evolution of the D_2 deformation is interpreted as a strong vertical shortening associated with preferentially top to the East shearing, which occurred synchronously with substantial decompression (Baudin & Marquer 1993). This progressive deformation induces crustal thinning with a stretch parallel to the Alpine chain

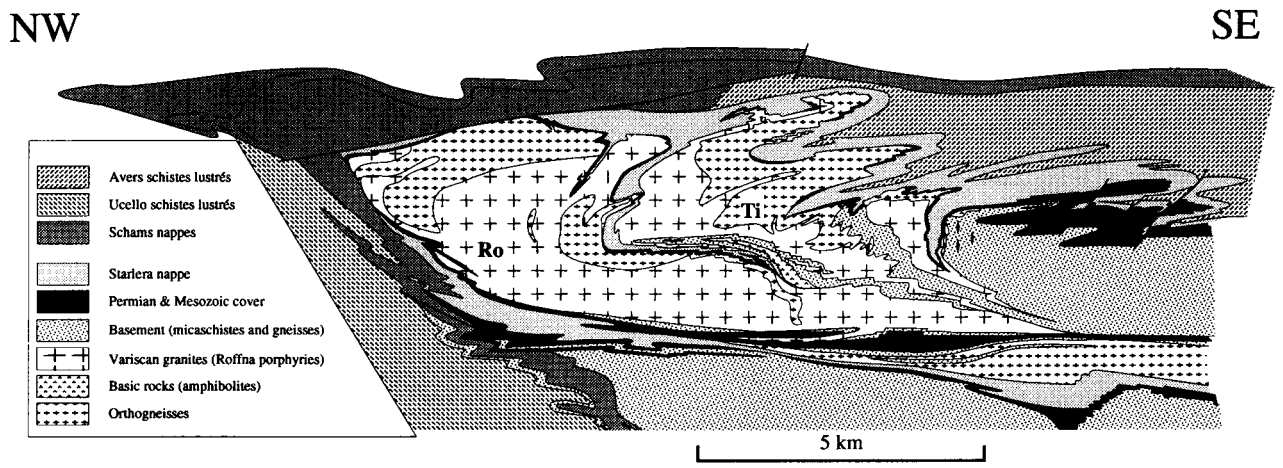

Fig. 3. NW–SE geological cross-section corresponding to the mapped area (Fig. 2) Ro: Roffna slice; Ti: Timun slice.

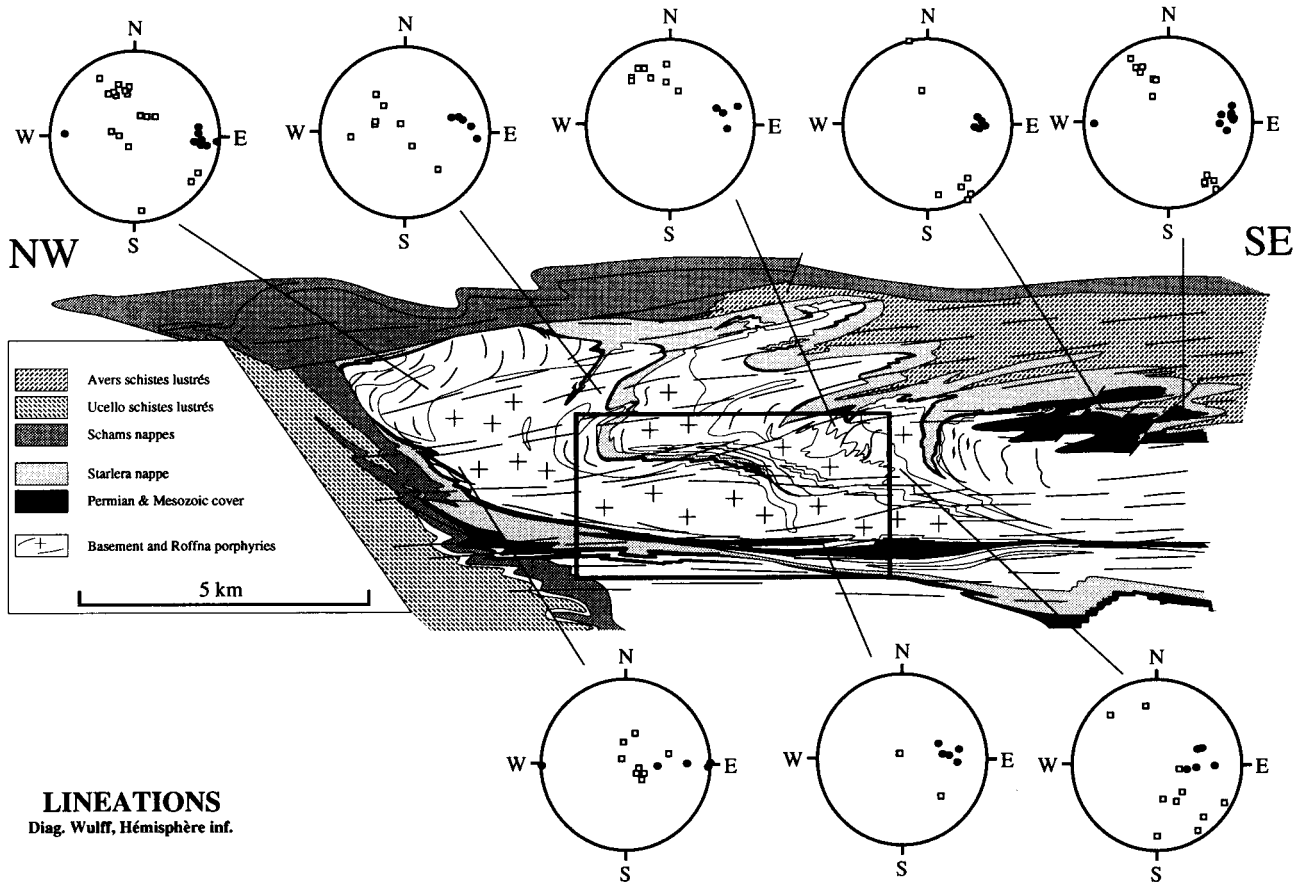

Fig. 4. NW–SE structural cross-section with the projection of the large scale D_2 shear zones trajectories (broken line) and distribution of weakly deformed areas in the Roffna granite (crosses). Stereographic projection of the Alpine stretching lineations in different parts of the nappe: D_1, squares; D_2, black dots. Rectangle corresponds to the location of the cross-section in Fig. 6.

during the lower Oligocene (Marquer *et al.* 1994). In this model, it is important to note that D_2 W–E stretching was still active in the upper Penninic nappes while the lower Penninic nappes were progressively transported towards the NNW. Moreover D_2 thinning could also explain a part of the exhumation of the eastern part of the high grade Ticino zone (Bradbury & Nolen-Hoeksema 1985, Deutsch *et al.* 1985, Hurford 1986, Hurford *et al.* 1989, Merle 1994).

The subsequent deformation events, D_3 and D_4, have not strongly modified the overall structure of the nappe pile. These deformations occurred under lower greenschist facies conditions and became much more localised. D_3 deformation is expressed by E–W trending rhythmic folds with a 'staircase' geometry at the nappe scale (Baudin *et al.* 1993). This north-vergent D_3 folding is possibly linked to the uplift along the Insubric line (Marquer *et al.* 1994). D_4 deformation consists of several NNW–SSE brittle–ductile normal faults, steeply dipping towards the ENE and lowering the eastern sides with hectometric fault throws. This late D_4 extensional deformation seems to be a symmetrical structure coeval with

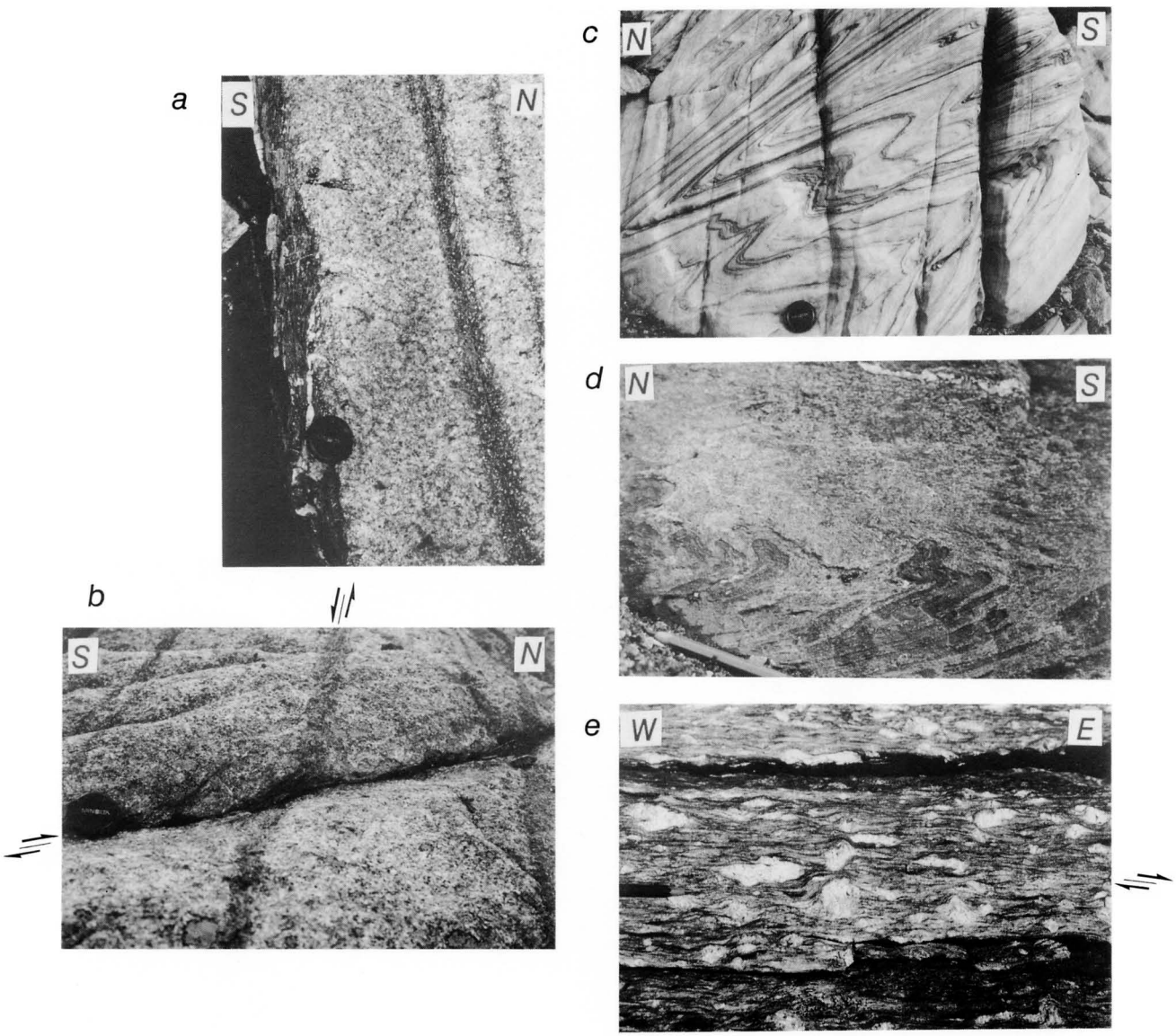

Fig. 5. Examples of typical studied structures and microstructures. (a) Shear zone in the Roffna granite used as shear criteria (C/S relationships, Berthé *et al.* 1979). (b) Conjugate shear zones in the Roffna granite defining a small scale shear zone pattern. (c) Isoclinal folds in Triassic sediments from the Starlera nappe at the top of the Roffna slice. (d) Superposed folding in the calcschistes of the autochthonous cover of Suretta at the top of the Roffna slice. (e) Shear band microstructures used as shear criteria in old orthogneisses (D_2). Scales are given by lens cover or pencils.

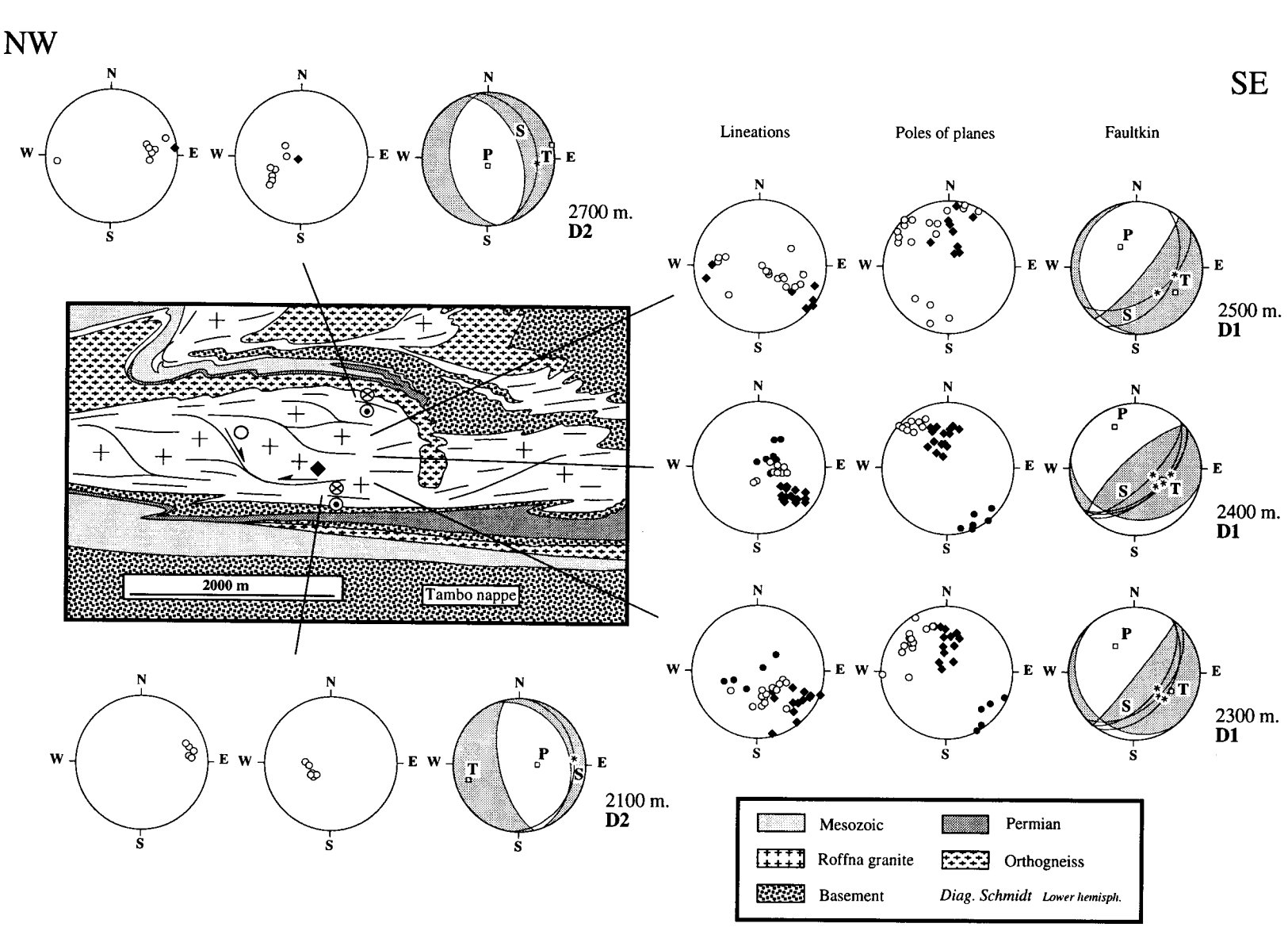

Fig. 6. Shear zone patterns of D_1 and D_2 deformation in the Roffna slice. Locations of measurement stations on a vertical simplified geological cross-section with the corresponding altitudes. For each location, stereographic projections illustrate the pattern of the dominant deformation: lineations, poles of shear zones planes and kinematic analysis are represented. Two conjugate sets are shown: a right hand shear sense set (viewed to the East), with open circles corresponding to normal ductile shear zones and dark circles to zones with southward sense of shear. A left hand shear sense set corresponding to shear zones with northward sense of shear (black squares). Kinematic analysis is performed using the shear zone planes/stretching lineations pairs, according to the method of Angelier & Mechler (1977) and Allmendinger *et al.* (1989). P and T are compression and tension axis respectively (white squares). Great circles (S) and stars on 'Faultkin' diagrams correspond to schistosity and associated lineation, respectively, measured in the middle of weakly deformed lenses.

the last Simplon normal faulting (Mancktelow 1985, Steck 1984, 1990) and could also be linked to late transpression of the Apulian plate along the Alpine arc (Schmid & Froitzheim 1993).

HETEROGENEOUS DEFORMATION AT THE NAPPE SCALE

Geometry of the main ductile deformations in the Suretta nappe

In this area, the early Tertiary deformation starts with décollement tectonics which leads to Mesozoic cover nappes (Starlera phase, see Baudin & Marquer 1994) overlying the reduced autochthonous cover. This early thin-skinned tectonics is also described in overlying equivalent structural units of the western Swiss Alps (Sartori 1990). This upper crustal deformation stage is followed by the stacking history and the burying of the Pennine nappes. In this paper, we only consider the two main ductile deformation phases, D_1 and D_2, which developed under greenschist facies conditions in the northern part of the Suretta nappe. During progressive D_1 and D_2 deformations, the types of structures recorded in basement and cover were different (Baudin & Marquer, 1994).

(1) In the basement, the geometry of structures is governed by very heterogeneous deformation leading to shear zones surrounding lenses of weakly deformed rocks (Figs. 5a & b). In these zones, pre-Alpine structures are recognisable and intrusive contacts or magmatic structures are well-preserved in the Roffna granite (crosses on Fig. 4). The Suretta nappe comprises two different basement slices, separated by a continuous layer of Mesozoic cover. The frontal slice is mainly composed of Roffna granite (the Roffna slice, Fig. 3) whereas the overlying southern slice is constituted by a large part of old basement (the Timun slice, Fig. 3). This geometry results from the D_1 deformation. Large scale D_2 ductile shear zones, recognized in the field, are projected in a NW–SE cross-section (Fig. 4). These principle zones of intense deformation, well-defined in the Suretta basement, may be traced into the cover, where intensely folded domains are predominant. For example, the large D_2 shear zones are responsible for the famous refolding of the previously stacked structures, mainly located in an area corresponding to the frontal part of the Timun slice in the Piz Grisch-Ferrera valley at the top of the Suretta nappe (Fig. 4) (Niemet–Beverin phase: Milnes & Schmutz 1978, Schmid *et al.* 1990, Schreurs 1993).

(2) On the other hand, the cover has undergone much more penetrative deformation, characterised by locally intense folding (Fig. 5c). During the first deformation, isoclinal curviplanar folds were developed leading to fold axes parallel to the NW–SE stretching lineations in the vicinity of the main D_1 thrusts. In the studied area, the previous contacts between the basement and the cover were strongly affected by the D_2 deformation (Fig. 4). This second deformation phase is linked to a gently E-dipping schistosity with a strong E–W stretching lineation and led to superimposed structures with D_2 fold axes trending NE–SW to E–W in zones of high strain (Fig. 5d). The D_2 folds in the cover are mainly SE vergent. This geometrical relationship between D_2 fold axes subparallel to E–W stretching lineation and systematic SE vergent folding is interpreted as the result of the refolding of old foliations dipping towards the SE as a consequence of D_1 thrusting (Baudin *et al.* 1993). The kinematics of D_2 deformation is deduced from asymmetrical microstructures, indicating predominant top to the East senses of shear which are particularly well-developed in orthogneisses of the basement (Fig. 5e)

Strain distribution in the Roffna granite

In the northern part of the Suretta nappe, the late Variscan Roffna granite (see Grunenfelder 1956) shows a heterogeneous strain (Figs. 5a & b). The following analysis of shear zone patterns focuses on the frontal slice of Suretta nappe because of the occurrence of the monocyclic Roffna granite in a continuous outcrop from the bottom to the top of the Roffna slice (Fig. 6). In the studied area, the Roffna slice was unaffected by the large scale refolding present at the upper contact of the Suretta nappe (Fig. 4) and thus earlier structures are not back-rotated. The geometry of the deformation is characterised by ductile shear zones surrounding lenses of weakly deformed granite (Fig. 5b). Heterogeneous deformation is present at all scales (see cross-sections in Figs. 4, 6 and 5b). In some small areas, the magmatic xenolith fabric is well-preserved and relicts of the previous magmatic deformations are found corresponding mainly to a weak magmatic foliation with N120–N140 strikes and subvertical dips.

A weak schistosity and stretching lineation occurs in the core of the lenses and become intense close to the shear zones. The analysed shear zones were high strain zones contemporaneous with major ductile deformations and metamorphism. Shear zones formed during D_1 or D_2 deformation have been distinguished in the field by using superimposed structures and the geometry of schistosity planes and stretching lineations associated with these differently oriented shear zones. In other words, all the measured shear zones were attributed to D_1 or D_2 deformation with respect to relative chronological criteria, and the measured direction of the main principal axis, X, present on the schistosity for each deformation phase (e.g. X direction, NW–SE for D_1 and E–W for D_2 (Fig. 4)). Shear zone patterns have been analysed every 100–200 m on a continuous vertical profile. The results of this analysis reveal that the first deformation is well-developed within the entire slice. The second deformation, however, is more pronounced in the basal and upper parts (Fig. 6, D_1/D_2): D_2 deformation is intense (Fig. 5e) and well-localized at the boundaries of the slice, around 2100 m and 2700 m. Between 2100 m and 2300 m D_1 and D_2 are present,

while between 2500 m and 2700 m the Roffna granite is only weakly deformed by D_1 deformation.

Geometry of shear zone patterns

For each shear zone pattern, the description of poles of shear zone planes, stretching lineations and shear senses derived from classical shear criteria analysis (Figs. 5a, b & e) provide the following results: from 2300 m to 2500 m, the regional D_1 schistosity (X/Y) was measured in the weakly deformed lenses and shows a constant average N45° strike, parallel to the Y direction (great circles S in stereograms, Fig. 6). Both schistosity and associated stretching lineation (stars in stereograms, Fig. 6) dip toward the south-east. In all the studied areas, the shear zone patterns associated with D_1 deformation are represented by conjugate zones intersecting close to the Y direction. The first set consist of moderately dipping shear zones with a SE oriented stretching lineation and a top to the NW dominant shear sense (squares in Fig. 6). The second set is represented by steeply inclined shear zones, northwest or southeast dipping and associated with subvertical lineations (open and black circles in Fig. 6). These shear zones mainly lower the SE blocks, as shown in the core of the Roffna granite (cross-section, Fig. 6). These data show an equal distribution of these two conjugate sets in the stereograms, without any preferred set (Fig. 6).

On the contrary, at the top (2700 m) and bottom (2100 m) of the slice, D_2 deformation shows a dominant set corresponding to shear zones dipping slightly towards the east and indicating a top to the east shearing, very few conjugates with top to the west being present (Fig. 6, open circles and squares). The regional D_2 schistosity (X/Y) at the upper and lower margin of the Roffna granite is subhorizontal or close to the dominant set of shear zones (great circles S on stereograms, Fig. 6). The associated stretching lineations are dipping toward the east (stars on stereograms, Fig. 6).

Shear zone patterns and fault kinematic analysis

Tectonic studies traditionally focus either on brittle deformation by looking at fault populations (Engelder & Geiser 1980, Angelier 1984, Hancock 1985, Marrett & Allmendinger 1990), or on ductile deformation by analysing shear zone patterns (Gapais *et al.* 1987, Marquer 1990, 1991). These two approaches, with their own methods, have caused controversy in their interpretation in terms of strain and/or stress for several decades. One recent paper about the use of 'shear zones as a new type of palaeostress indicator' (Srivastava *et al.* 1995) emphasises the importance of comparing and applying brittle field methods to strain markers in brittle–ductile and ductile shear zones. Even if this interpretation in terms of palaeostress could be a source of debate, a careful analysis of the geometry and the kinematics of shear zone patterns and a comparison with principal axes deduced from the same shear zone populations using methods of fault plane analysis would allow new insights into the ductile shear zone analysis. In this paper, the method of fault kinematic analysis is applied to ductile shear zones and the resulting main stress axes (P and T axes) will be compared with strain axes (Z and X axes) deduced from classical strain analysis, using schistosity-stretching lineation couples measured in the lenses between the shear zones (Fig. 6, Faultkin). In our study, the P and T directions deduced from fault plane analysis do not represent stress axes but they are only used as a graphical representation to test the geometrical compatibility of shear zones.

In all the localities of D_1 deformation, the stretching lineation lying on the schistosity plane measured in the middle of weakly deformed lenses, corresponding to low strain domains, are close to the T (tension) axis (Fig. 6). In these diagrams, the schistosity planes are close to the plane containing the T axis and the intermediate axis of the fault kinematic solution. In that case, the schistosity acts as a symmetrical plane between the two sets of shear zones. The agreement between measured principal axes (schistosity X-Y, great circles with stars in Fig. 6, lineation X, stars in Fig. 6) and fault kinematic results attests for a good compatibility of the shear zones and the schistosity and confirms the NW–SE shortening during D_1.

On the other hand, the fault kinematic analysis for D_2 shear zones reveals an asymmetry of the position of the D_2 schistosity (X-Y, great circles with stars in Fig. 6) with respect to the calculated extension field (dashed area, Fig. 6). An obliquity of the dip of the stretching lineation (X, stars in Fig. 6) with respect to the T axis is also observed. In these diagrams, the D_2 schistosity is close to a great circle delimiting the Tension/Compression fields. The schistosity is always at low angle to the dominant set of shear zone (open circles, Fig. 6). Even if their dips differ slightly, the stretching lineation and the T axis trend in the same E–W direction, while the shortening is almost vertical (Fig. 6). These symmetrical/asymmetrical results are used as large-scale kinematic indicators to establish the bulk strain regime of a crustal structure (Choukroune *et al.* 1987).

Bulk kinematics

Using the geometry of the tectonic contacts at the boundary of the nappe for D_1 and D_2 deformation, the results provided by shear zone pattern analyses at the scale of measurement stations can be interpreted in terms of bulk kinematics, strain intensity and strain localisation at the nappe scale. The D_1 and D_2 shear zone patterns in the different areas of the Roffna slice, lead to symmetric/asymmetric patterns versus schistosity, lineation and T–P axes which are interpreted as non-coaxial deformation in low strain domains for D_1 deformation (Fig. 7, S, L and T on the same axis) and non-coaxial deformation in high strain domains for D_2.

For this D_2 deformation, the schistosity and stretching lineation measured in the field (S, L in Fig. 7) are located in the tension field of fault kinematic analysis, but are close to the dominant set of shear planes (open circles in Fig. 7) and not close to the dihedral symmetric plane containing the T and intermediate axes of the fault kinematic analysis (T on Fig. 7). This asymmetrical geometry is interpreted as a strongly non-coaxial deformation at this scale (Fig. 7). In these two cases, we suggest that the orientation of P and T axes, calculated with the shear zone pattern analyses, are close to the principal axes of the incremental strain ellipsoid (dashed ellipsoid in Fig. 7) while the schistosity and the stretching lineation measured in the field correspond to the principal axes of the finite strain ellipsoid. With such interpretation, finite strain and incremental strain ellipsoids are parallel for D_1 and oblique for D_2 deformation. Such features could be related to the low and widely distributed strain observed for D_1 whereas the D_2 deformation geometry reflects higher strained domains, strongly localised at the bottom and top of the Roffna slice. At the scale of the Roffna slice, the bulk asymmetry of the D_1 and D_2 shear zone patterns in the Roffna granite compared to the mainly horizontal or gently east dipping tectonic contacts is interpreted as a C/S relationship, and confirms the kinematics recorded by these contacts or by other Penninic nappes in this area (large black arrows on Fig. 7): D_1 corresponds to a stacking of the nappe towards the NW and is followed by D_2 with a top to the E shearing.

CONCLUSIONS

This approach allows us to draw conclusions about the geometry, the distribution and the kinematics of basement deformation. Because the main contacts between tectonic units are often reworked in collision belts, and because observations of local kinematic indicators reveal only late tectonic events, the analysis of shear zone patterns at the scale of a nappe is a powerful instrument in order to deduce the bulk kinematics. The comparison between the orientation of P–T axes resulting from shear zone pattern analysis using fault kinematics and the direction of the principal strain axes defined by schistosity and stretching lineation allows a description of the kinematics and the distribution of the two main ductile deformations recorded from the bottom to the top of the Roffna granite. The first phase, well expressed in the whole nappe, corresponds to a top to the northwest sense of shear and the second phase, preferentially developed at the top and the bottom of the nappe, indicates a top to the east sense of shear. The deformed granites provide a powerful strain marker and kinematic indicator at the bulk scale.

The study of shear zone patterns and strain distribution at the nappe scale is a tool to understand the basement behaviour during collisional building processes. The basement rocks seem to be mainly controlled by heterogeneous deformation while the cover is mainly affected by large scale folding. This heterogeneous and localised deformation expressed in the

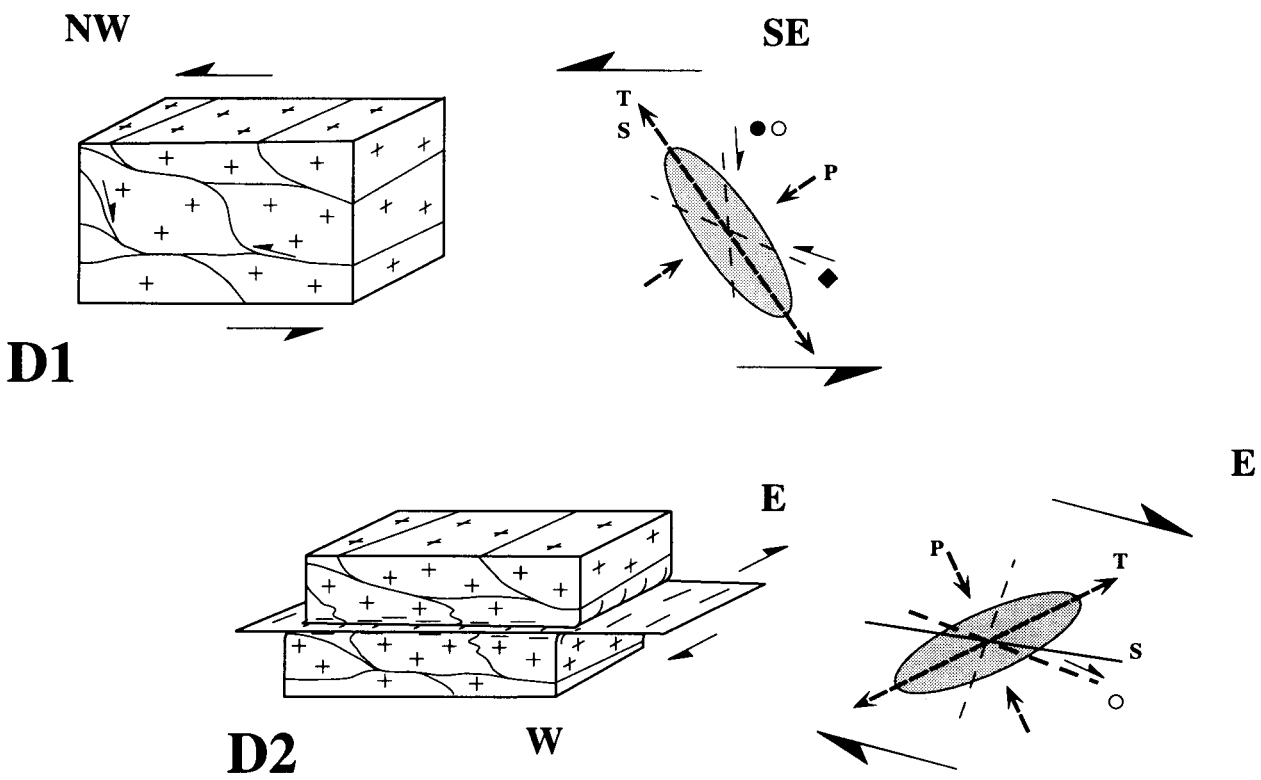

Fig. 7. Sketch of the kinematic interpretation of D_1 and D_2 deformations. The shearing plane (large arrows) corresponds to orientation of the main tectonic boundaries of the nappe. Circles, squares and stars are as in Fig. 6. P and T are the calculated compression and tension axis using Faultkin (Fig. 6). S is the average of schistosity and lineation measured in the field (Fig. 6); their orientations are compared with P–T axis, see text for explanations.

basement nappes leads to large preserved domains which are of importance to the reconstruction of the tectono-metamorphic history of these old basement units.

Acknowledgements—This work was supported by Swiss National Founds, FNSRS No: 20.33421-92. Thanks to S. Schmid and an anonymous reviewer for suggesting significant improvements to this paper.

REFERENCES

Allmendinger, R. W., Marrett, R. A. & Cladoulos, T. 1989. Fault kinematics: a program for analysing fault slip data for the Macintosh computer. Cornell University, Ithaca.

Angelier, J. 1984. Tectonic analysis of fault slip data sets. *J. geophys. Res.*, **89**, 5835–5848.

Angelier, J. & Mechler, P. 1977. Sur la méthode graphique de recherche des contraintes principales également utilisable en tectonique et en seismologie: la méthode des dièdres droits. *Bull. Soc. géol. France*, **XIX**, 1309–1318.

Argand, E. 1911. Les nappes de recouvrement des Alpes Penniques et leur prolongements structuraux. *Matér. Carte géol. Suisse N.S.* **31**.

Argand, E. 1916. Sur l'arc des Alpes Occidentales. *Eclogae geol. Helv.* **14**, 145–191.

Baudin, Th. & Marquer, D. 1993. Histoire P–T-déformation du socle et de la couverture de la nappe de Tambo: utilisation du géobaromètre phengitique (Alpes centrales suisses). *Schweiz. Miner. Petrogr. Mitt.* **73**, 293–307.

Baudin, Th., Marquer, D. & Persoz, F. 1993. Basement–cover relationships in the Tambo nappe (Central alps, Switzerland); geometry, structures and kinematics. *J. Struct. Geol.* **15**, 543–553.

Baudin, Th. & Marquer, D. 1994. Comparaison des relations socle-couverture entre les zones internes et externes dans les Alpes centrales. *Schweiz. Miner. Petrogr. Mitt.* **74/3**, 453–458.

Baudin, Th., Marquer, D., Barfety, J. C., Kerckhove, C. & Persoz, F. 1995. A new stratigraphical interpretation of the mesozoic cover of the Tambo and Suretta nappes: Evidence for early thin-skinned tectonics. *C. R. Acad. Sci. Paris* **321**, 401–408.

Bell, T. H. 1981. Foliation development: the contribution, geometry and significance of progressive bulk, inhomogeneous shortening. *Tectonophysics* **75**, 273–296.

Berthé, D., Choukroune, P. & Jégouzo, P. 1979. Orthogneiss, mylonite and non co-axial deformation of granites: example of the south armorican shear zone. *J. Struct. Geol.* **1**, 31–42.

Bradbury, H. J. & Nolen-Hoeksema, R. C. 1985. The lepontine Alps as an evolving metamorphic core complex during A-Type subduction: Evidence from heat flow, mineral cooling ages, and tectonic modeling. *Tectonophysics* **4**, 187–211.

Choukroune, P. & Gapais, D. 1983. Strain pattern in the Aar granite (Central Alps): orthogneiss developed by bulk inhomogeneous flattening. *J. Struct. Geol.* **5**, 411–418.

Choukroune, P., Gapais, D. & Merle, O. 1987. Shear criteria and structural symmetry. *J. Struct. Geol.* **9**, 525–530.

Deutsch, A. & Steiger, R. H. 1985. Hornblende, K–Ar and the climax of Tertiary metamorphism in the Lepontine Alps (South Central Switzerland); an old problem reassessed. *Earth Planet. Sci. Lett.* **72**, 175–189.

Engelder, T. & Geiser, P. 1980. On the use of regional joint sets as trajectories of palaeostress fields during the development of the Appalachian plateau. *J. geophys. Res.* **85**, 6319–6341.

Escher, A., Masson, H. and Steck, A. 1993. Nappe geometry in the Western Swiss Alps. *J. Struct. Geol.* **15**, 501–509.

Frei, W., Heitzmann, P., Lehner, P., Muller, St., Olivier, R., Pfiffner, A., Steck, A. & Valasek, P. 1989. Geotraverses across the Swiss Alps. *Nature* **340**, 544–548.

Frey, M., Hunziker, J. C., Frank, W., Bocquet, J., Dal Piaz, G. V., Jäger, E. & Niggli, E. 1974. Alpine metamorphism of the Alps: a review. *Schweiz Miner. Petrogr. Mitt.* **54/2/3**, 277–290.

Frey, M., Bucher, K., Frank, E. & Mullis, J. 1980. Alpine metamorphism along the geotraverse Basel–Chiasso: a review. *Eclog. geol. Helv.* **73**, 527–546.

Gapais, D., Balé, P., Choukroune, P., Cobbold, P., Mahdjoub, Y & Marquer, D. 1987. Bulk kinematics from shear zone patterns; some field examples. *J. Struct. Geol.* **9**, 635–646.

Grünenfelder, M. 1956. Petrographie des Roffnakristallins in mittelbünden und seine eisenvererzung. *Beitr. Geol. Karte Schweiz* **35**.

Hancock, P. L. 1985. Brittle microtectonics, principles and practice. *J. Struct. Geol.*, 7, 437–457.

Hurford, A. J. 1986. Cooling and uplift patterns in the Lepontine Alps, South Central Switzerland and an age of vertical movement on the Insubric fault line. *Contr. Miner. Petrol.* **92**, 413–427.

Hurford, A. J., Flisch, M. & Jäger, E. 1989. Unravelling the thermotectonic evolution of the Alps: a contribution from fission track analysis and mica dating. In: *Alpine Tectonics* (edited by Coward M., Dietrich D. & Park, R.). *Spec. Publs. geol. Soc. Lond.* **45**, 369–398.

Mancktelow, N. 1985. The Simplon line: a major displacement zone in the western Lepontine Alps. *Eclog. geol. Helv.* **78**, 73–96.

Marquer, D. 1990. Structures et deformation alpine dans les granites Hercyniens du massif du Gothard (Alpes Centrales Suisses) *Eclog. geol. Helv.* **83/1**, 77–97.

Marquer, D. 1991. Structures et cinématique des déformations Alpines dans le granite de Truzzo (Nappe de Tambo: Alpes Centrales Suisses). *Eclog. geol. Helv.* **84/1**, 107–123.

Marquer, D. & Peucat, J. J. 1994. Rb/Sr systematics of recrystallized shear zones at the greenschist–amphibolite transition: examples from granites in the Swiss Central Alps. *Schweiz. Miner. Petrogr. Mitt.* **74/3**, 343–358.

Marquer, D., Baudin, T., Peucat, J. J. & Persoz, F. 1994. Rb–Sr micas ages in the Alpine shear zones of the Truzzo granite: The timing of the Tertiary alpine P–T-deformations in the Tambo nappe (Central Alps, Switzerland). *Eclog. geol. Helv.* **87/1**, 225–240.

Marrett, R. & Allmendinger, R. 1990. Kinematic analysis of the fault slip data. *J. Struct. Geol.* **12**, 973–986.

Massonne, H. J. & Schreyer, W. 1987. Phengite geobarometry based on the limiting assemblage with K-feldspar, phlogopite, and quartz. *Contr. Miner. Petrol.* **96**, 212–224.

Mayerat, A. M. 1994. Analyse structurale de la zone frontale de la nappe de Tambo (Pennique, Grisons, Suisse). *Mat. Carte Géol. Suisse NS* **165**, 68 p.

Merle, O. 1994. Syn-convergence exhumation of the Central Alps. *Geodinamica Acta* **7**, 129–138.

Merle, O., Cobbold, P. R. & Schmid, S. 1989. Tertiary kinematics in the Lepontine dome. In: *Alpine tectonics* (edited by Coward M., Dietrich D. & Park, R.). *Spec. Publs. geol. Soc. Lond.* **45**, 113–134.

Milnes, A. G. & Schmutz, H. U. 1978. Structure and history of the Suretta nappe (Pennine zone, Central Alps): A field study. *Eclog. geol. Helv.* **71/1**, 19–33.

Mitra, G. 1978. Ductile deformation zones and mylonites; The mechanical processes involved in the deformation of crystalline basement rocks. *Am. J. Sci.* **278**, 1057–1084.

Mitra, G. 1979. Ductile deformation zones in Blue Ridge basement rocks and estimation of finite strains. *Bull. geol. Soc. Am.* **90**, 935–951.

Pfiffner, O. A., Frei, W., Finckh, P. & Valasek, P. 1988. Deep seismic reflection profiling in the Swiss Alps: Explosion seismology results for line NFP-20East. *Geology* **16**, 987–990.

Pfiffner, O. A., Klaper, E. M., Mayerat, A. M. & Heitzmann, 1990. Structure of the basement–cover contact in the Swiss Alps. *Mém géol. Soc. Suisse* **1**, 247–262.

Ramsay, J. G. & Allison, I. 1979. Structural analysis of shear zones in an Alpinised Hercynian granite (Maggia Lappen, Pennine zone, Centrals Alps). *Schweiz. Miner. Petrogr. Mitt.* **59**, 251–279.

Sartori, M. 1990. L'unité du Barrhorn (Zone Pennique, Valais, Suisse). *Mémoires de géologie*, Lausanne, **6**, 157 pp.

Schmid, S. M. & Froitzheim, N. 1993. Oblique slip and block rotation along the Engadine line. *Eclog. geol. Helv.* **86/2**, 569–593.

Schmid, S. M., Rück, P. & Schreurs, G. 1990. The significance of the Schams nappes for the reconstruction of the paleotectonic and orogenic evolution of the Penninic zone along the NFP-20East traverse (Grisons, Eastern Switzerland). *Mém géol Soc. Suisse* **1**, 263–287.

Schreurs, G. 1993. Structural analysis of the Schams nappes and adjacent tectonic units: implications for the orogenic evolution of the Penninic zone in the Eastern Switzerland. *Bull. géol. Soc. France* **164**, 425–435.

Srivastava, D. K., Lisle, R. J. & Vandycke, S. 1995. Shear zones as a new type of paleostress indicator. *J. Struct. Geol.* **17**, 663–676.

Staub, R. 1916. Zur Tektonik der Südostlichen Schweizeralpen. *Beitr. geol. Karts Schweiz N.F.* **46**, 198 pp.

Staub, R. 1924. Der Bau der Alpen. *Beitr. geol. Karte Schweiz N.F.* **52**.

Steck, A. 1984. Structures de déformations Tertiaires dans les Alpes Centrales (transversale Aar-Simplon-Ossola). *Eclog. geol. Helv.* **77**, 55–100.

Steck, A. 1990. Une carte des zones de cisaillement ductile des Alpes Centrales. *Eclog. geol. Helv.* **83**, 603–627.

Steinmann, M. 1994. Ein Beckenmodell für das Nordpenninikum der Ostschweiz. *Jb. Geol. B.-A.* **137/4**, 675–721.

Streiff, V., Jäckli, H. & Neher, J. 1976. *Atlas géologique de la Suisse 1:25000, 1235 Andeer, Comm. géol. Suisse.* **56**.

Trumpy, R. 1980. Geology of Switzerland, a guide book. In: *Part A: An Outline of the Geology of Switzerland. Schweiz. geol. Komm. Eds Wepf & Co, Basel.*

Wilhelm, O. 1933. Geologie de Landschaft Schams (Graubünden). *Beitr. geol. Karte Schweiz NF* **64**, 1–32.